Chapter 7

Low dystrophin levels increase survival and improve muscle pathology and function in dystrophin/utrophin double knockout mice

M. van Putten, M. Hulsker, C. Young, V.D. Nadarajah, H. Heemskerk, L. van der Weerd, P.A.C. 't Hoen, G.J.B. van Ommen, A.M. Aartsma-Rus

Submitted

Abstract

Duchenne muscular dystrophy is a severe muscle wasting disorder caused by the lack of functional dystrophin. There is no cure, but several clinical trials are underway aimed at restoring the synthesis of functional dystrophin. The dystrophin levels needed for improvement of muscle pathology, function and overall vitality are unknown. Here, we describe the *mdx/utrn*$^{-/-}$*/Xist*$^{\Delta hs}$ mouse model, which expresses a range of low dystrophin levels depending on the degree of skewing of X-inactivation in a utrophin negative background. *Mdx/utrn*$^{-/-}$ mice develop severe muscle weakness, kyphosis, respiratory and heart failure and premature death closely resembling DMD pathology. We show that dystrophin levels below 4% already greatly improve survival and motor function in these animals. In mice expressing more than 4% dystrophin, histopathology is ameliorated as well. This suggests that the dystrophin levels needed to benefit vitality and functioning of DMD patients might be lower than those needed for full protection against muscle damage.

Introduction

Duchenne muscular dystrophy (DMD) is the most common inherited neuromuscular disorder. It is caused by mutations which disrupt the reading frame of the *DMD* gene located on the X-chromosome. These mutations result in a premature stop codon, which prevents the synthesis of functional dystrophin (Hoffman et al. 1987). Dystrophin provides muscle fiber stability during contraction by anchoring the extracellular matrix to actin filaments. When this connection is absent, fibers are vulnerable to exercise-induced damage and, upon exhaustion of the regenerative capacity, they will be replaced by fibrotic and fat tissue. The continuous loss of muscle tissue results in loss of ambulation generally in the second decade of the patient's life. Due to improved care including corticosteroid treatment, spinal surgery and assisted ventilation, patients now survive till the third or forth decade in the Western world (Muntoni et al. 2003;Kohler et al. 2009). Mutations that do not disrupt the reading frame are found in Becker muscular dystrophy patients (BMD). These patients express dystrophin of lower quantity and/or of different quality (generally internally deleted) that is partly functional, resulting in a milder phenotype.

The *mdx* mouse is the most commonly used mouse model for basic and therapy research for DMD. It carries a nonsense/stop mutation in exon 23 of the mouse *Dmd* gene and consequently, like DMD patients, lacks functional dystrophin. The phenotype of this mouse is, however, less severe than that of DMD patients and the life span is nearly normal (Sicinski et al. 1989;Stedman et al. 1991). This is likely due to a better regenerative capacity than human muscle, as suggested by the upregulation of muscle transcription factors. Also the dystrophin homologue utrophin, in the mouse, seems better capable of replacing dystrophin. *Mdx/utrn*$^{-/-}$ mice, lacking both dystrophin and utrophin, mimic the DMD patients' phenotype more closely, since they are severely affected, develop kyphosis, show breathing difficulties and do not live beyond 3 months (Deconinck et al. 1997b, Grady et al. 1997a).

There is no cure for DMD, but several therapeutic approaches, aiming to restore the expression of functional dystrophin, are currently under investigation in clinical trials (Goemans et al. 2011;Cirak et al. 2011;Bowles et al. 2011;Malik et al. 2010;Skuk et al. 2006). It is, however, unknown which dystrophin levels are needed to obtain a beneficial effect in DMD patients and whether correction of muscle function, histopathology and overall vitality require similar dystrophin levels.

Previously, two attempts have been undertaken to elucidate this. The *mdx*^{3cv} mice (expressing ~5% of truncated dystrophin lacking exon 65/66) were crossed into two different utrophin negative backgrounds (Rafael et al. 1999;Li et al. 2010). In the first study, these mice

were as severely affected as *mdx/utrn*$^{-/-}$ mice and no increase in the 12-week life span was observed. By contrast, (Li et al. 2010) the other study reported mice with a median survival of 79 weeks. Despite discrepancies between these models, their common drawback is that dystrophin expression is limited to <5% of a compromised dystrophin in the *mdx*^{3cv} model, whereas expression of a broader range of a partially functional dystrophin is preferred.

We here determined the effects of a broad range of low dystrophin levels against an *utrn*$^{-/-}$ background on muscle integrity, pathology, function and overall viability in the *mdx/utrn*$^{-/-}$*/Xist*$^{\Delta hs}$ mouse model. These mice have mutations in the *Xist* gene of one X-chromosome leading to skewed X-inactivation, combined with a defective dystrophin on the other X-chromosome, resulting in low dystrophin levels (Newall et al. 2001). Introducing low, but varying, dystrophin levels resulted in improvements in life span and pathology, ranging from that of severely affected *mdx/utrn*$^{-/-}$ to almost wild type mice. Dystrophin expression correlated with survival and severity of pathology: where <4% dystrophin already significantly improved life span and muscle function, levels of >4% dystrophin not only further improved this, but also protected muscles against damage.

Materials and methods

Animal care

All mice participating in this study were bred at the animal facility at the LUMC where they were housed in groups in individually ventilated cages with 12-h light-dark cycles. Mice were given standard chow and water *ad libitum*. The generation of *mdx/utrn*$^{-/-}$*/Xist*$^{\Delta hs}$ mice was performed in two steps. First, we crossed *Xist*$^{\Delta hs}$ females (Newall et al. 2001) with *hDMD*$^{+/-}$*utrn*$^{-/-}$ males. The *hDMD* mouse has an intact and functional copy of the human dystrophin gene, which can functionally compensate for the lack of mouse dystrophin ('t Hoen et al. 2008). Offspring were genotyped, and *utrn*$^{+/-}$*/Xist*$^{\Delta hs}$ mice lacking the *hDMD* gene were interbred to generate *utrn*$^{-/-}$*/Xist*$^{\Delta hs}$ mice. *Utrn*$^{-/-}$*/Xist*$^{\Delta hs}$ males were then crossed with *mdx/utrn*$^{+/-}$ females, giving rise to female *mdx/utrn*$^{-/-}$*/Xist*$^{\Delta hs}$ mice, which were used for experiments (Fig. 1A). The *Xist*$^{\Delta hs}$ mice were a kind gift from Prof. Brockdorff (MRC Clinical Sciences Centre London, UK, current affiliation Department of Biochemistry, University of Oxford, UK). Genotyping was performed on DNA obtained from ear biopsies by PCR analysis (primers and PCR conditions available on request). All experiments were approved by the Animal Experimental Committee (DEC) of the LUMC. Mice that became too severely affected (body weight drop of >15% within two days) were sacrificed. All mice used in the study were females, except for the *mdx/utrn*$^{-/-}$ mice of which both genders were used.

Determination of functional performance

To assess forelimb grip strength, mice were suspended above the grid of a strength meter (Columbus Instruments, USA), which they instinctively grasped and were then pulled backwards forcing release of the grid. Five measurements were made in a row and the average of the three highest measured values was divided by the body weight in grams and used for further analysis.

To determine running performance on the rotarod (Ugo Basile, Italy), mice were placed on the rotating tube, which accelerated from 5 to 45 rotations per min within 15 sec. Mice had to run for a maximum of 500 sec without falling. Individuals that fell off earlier were given two more tries. The longest running time was used for analysis.

The two limb hanging wire test was conducted with a metal cloth hanger that was secured above a cage filled with bedding. Mice had to grasp the wire with the two forelimbs and were then released. During the 10 min session, all limbs and the tail were used depending on the

functional ability of the mouse. Mice that were not able to hang for the maximum time were allowed two more tries. Maximum hanging time was used for analysis.

For the four limb hanging wire test, mice were placed on a grid, which was turned upside down above a cage filled with bedding, forcing mice to hang using four limbs from the start of the test onwards. The session ended when the mice had hung for 10 min or otherwise after three sessions. Maximum hanging time was used for analysis. When possible, standardized operating procedures from the TREAT-NMD network were implemented (http://www.treat-nmd.eu/resources/research-resources/dmd-sops/).

Blood biomarker analysis

At the age of 8 and 14 weeks blood was collected via the tail to determine serum biomarker levels of matrix metallopeptidase-9 (MMP-9), tissue inhibitor of metalloproteinases-1 (TIMP-1) and vascular endothelial growth factor (VEGF) (Nadarajah et al. 2011;Saito et al. 2009). The mouse MMP-9 (total) immunoassay kit (catalog number MMPT90), mouse TIMP-1 immunoassay kit (catalog number MTM100) and mouse VEGF immunoassay kit (catalog number MMV00) were purchased from R&D systems (UK). Collected blood was allowed to clot at room temperature for 10 min before centrifuging (1700 x *g* for 10 min at 4°C) and stored at -80°C, before use. Age and gender-matched C57BL/10ScSnJ ($n = 4$) and *mdx/utrn*$^{-/-}$ mice ($n = 4$) were used as controls.

Plasma creatine kinase (CK) levels were determined in blood that was obtained via the tail and collected in a Minicollect tube (0.8ml Lithium Heparin Sep, Greiner bio-one, Austria). CK levels were determined with Reflotron CK test strips in the Reflotron plus machine (Roche diagnostics Ltd, UK).

Heart function assessment

Mice were transported to the Faculty of Science at the University of Leiden where they were housed for at least one week to acclimatize. Heart function was assessed by Magnetic Resonance Imaging (MRI) in a vertical 9.4T magnet with 89 mm bore size, equipped with a 1 T/m gradient system (Bruker BioSpin, Germany), using a quadrature birdcage coil with an inner diameter of 30 mm. Mice were anesthetized by inhalation of 2% isoflurane in a 1:1 mixture of oxygen and air. Respiratory rate was monitored during the scan with a respiratory pad and kept between 50-80 respirations per minute. Image acquisition was done with Bruker Paravision 5.0 software and took approximately 30 min per mouse including animal setup. A retrospectively-gated Intragate sequence was used with flip angle 10º; repetition time 8.5 ms; echo time 1.86 ms; field-of-view 2.56x2.56 cm^2; matrix 192x192; in-plane resolution 133 μm. We made 8-9 short-axis slices of the heart with a slice thickness of 1 mm and 200 repetitions per slice. The navigator echo was placed in-slice. Images were reconstructed to 18 frames per heart cycle. Scans were oriented on the left ventricle (Verhaart et al. 2011). Mice were sacrificed by cervical dislocation after completion of the scans. The scans were analyzed with MASS for MICE software (developed at the LUMC, Division of Image Processing (LKEB))(van der Geest et al. 1997;van der Geest and Reiber 1999). The endo and epicardial contours of both ventricles were drawn manually for each image. The end diastolic and systolic phase was computed by the software and a maximum mass difference of 10% was accepted for both ventricles. When this criterion was met, end diastolic and systolic volume were determined and based on these values stroke volume (end diastolic volume – end systolic volume), ejection fraction (stroke volume/end diastolic volume*100%) and cardiac output (stroke volume*heart rate) were calculated automatically. One *mdx/utrn*$^{-/-}$*/Xist*$^{\Delta hs}$ mouse was left out of the analysis as the scan was made with an incorrect angle.

Western blot analysis

Protein was isolated from the quadriceps and heart in 1 ml buffer (1.25 M Tris-HCl pH 6.8, 20% (v/v) glycerol and 25% (w/v) SDS) in MagNA Lyser green beads in the MagNA Lyser (Roche Diagnostics, the Netherlands). The BCA protein assay kit (Thermoscientific, Il, USA) was used according to the manufacturer's instructions to determine protein concentration. Subsequently, the protein solution was complemented with 5% (v/v) β-mercaptoethanol and 0.001% (w/v) bromophenol blue. The Trans-blot Turbo system (BioRad, the Netherlands) was used for Western blotting (Hulsker et al. manuscript in preparation). Samples (30 µg) were heated at 95°C for 5 min and 20 µl was loaded on 1.0 mm thick native PAGE Tris acetate (polyacrylamide) gels, with a linear resolving gel gradient of 3-8% (BioRad, the Netherlands). The gels were run on ice for 1 hr at 75 V (0.07 A) and 2 hrs at 150 V (0.12 A) in the running buffer (XT Tricine; BioRad; the Netherlands). When changing voltage, running buffer was refreshed to maintain pH. Proteins were blotted to membrane using the ready to use Trans-Blot Turbo transfer packs and the Trans-Blot Turbo transfer system at 2.5 A (25 V) for 10 min. Membranes were blocked for 1 hr with 5% (w/v) non-fat dried milk (Campina Melkunie, the Netherlands) in TBS and washed three times with TBST for 10 min. Primary dystrophin antibody NCL-DYS1 (dilution 1:125 in TBS, Novacastra, UK) and loading control α-actinin (dilution 1:5000 in TBS, AB72592, Abcam) were incubated overnight at 4°C. After the membranes were rinsed three times with TBS for 10 min, they were incubated for 1 hr with fluorescent IRDye 800CW goat-anti-mouse (dilution 1:5000, Li-Cor, NE, USA) and IRDye 650LT donkey-anti-rabbit (1:10,000, Li-Cor, NE, USA). Protein quantification was performed with the Odyssey system and software (Li-Cor, NE, USA).

Histological examination

After sacrifice, skeletal muscles and heart were dissected and snap frozen in 2-methylbutane (Sigma-Aldrich, The Netherlands) cooled in liquid nitrogen. For the quadriceps and heart, sections of 8 µm were cut along the entire length of the muscle with a Shandon cryotome (Thermo Fisher Scientific Co., Pittsburgh, PA, USA) with an interval of 240 µm between the sections. Sections of the quadriceps were stained with Harris Haematoxylin and Eosin (H&E), according to conventional histological procedures. From the middle section of the muscle, images covering the entire muscle were captured with a light microscope (Leica DM LB, Leica Microsystems, The Netherlands) and a Leica DC500 camera with Leica IM50 software (Leica Microsystems, The Netherlands) at a 5 times magnification. Blending and background correction was performed with Adobe Photoshop CS3 version 10.0.1. Freely available ImageJ software with the H&E colour deconvolution plugin (Rasband, W.S., ImageJ, U. S. National Institutes of Health, Bethesda, Maryland, USA, http://rsb.info.nih.gov/ij/) was used to determine the fibrotic/necrotic percentage of the entire cross-section by two individuals in a double blinded manner, as described previously (van Putten et al. 2010).

Fiber size and the percentage of centralized nuclei were determined with Mayachitra Imago 1 (http://www.mayachitra.com/imago/) (van Putten et al. manuscript in preparation) on five randomly captured images of the quadriceps stained with dystrophin (dilution 1:50, C-20, Santa Cruz, Germany) and laminin (dilution 1:50, ab11575, Abcam, UK) where donkey-anti-goat Alexa 594 and donkey-anti-rabbit Alexa 488 (dilution 1:1000, Invitrogen, the Netherlands) were respectively used as a secondary antibody. Slides were mounted with Vectashield mounting medium including DAPI (Vector Labs, Germany).

Cryosections of the heart were stained with goat-anti-Collagen type 1 (dilution 1:100, 1310-01 Southern Biotech, USA), rabbit-anti-goat Alexa 594 (dilution 1:1000, Invitrogen, The Netherlands) and DAPI. Sections were examined with a Leica DM RA2 fluorescent microscope at

a 16 times magnification and images covering the entire heart were captured with a Leica DC350FX snapshot camera. The percentage of fibrosis was quantified with ImageJ software (Rasband, W.S., ImageJ, U. S. National Institutes of Health, Bethesda, Maryland, USA, http://rsb.info.nih.gov/ij/).
Co-localization of dystrophin and β-dystroglycan was performed on a transverse cross-section of the quadriceps, stained with dystrophin (dilution 1:50, C-20, Santa Cruz, Germany) and β-dystroglycan (dilution 1:50, NCL β-DG, Novocastra UK). The staining was completed with donkey-anti-rabbit Alexa 488 (dilution 1:1000, Invitrogen, the Netherlands) and Fluorescein Avidin solution of the MOM kit (Vector Laboratories, UK), respectively.

RT-qPCR analysis

For total RNA isolation, tissue was disrupted in MagNA Lyser Green Beads tubes (Roche diagnostics Ltd, UK) with Tripure isolation reagent (Roche diagnostics Ltd, USA). Isolation was performed with chloroform, and RNA precipitated with isopropanol. The NucleoSpin RNA II kit including a DNAse digestion (Bioke, the Netherlands) was used for RNA purification. RNA integrity and concentration was checked with a total RNA nano-chip assay on a labchip bioanalyzer (Agilent, The Netherlands) and used for cDNA synthesis with random hexamer primers. Expression of genes involved in regeneration (*Myog*, *eMHC3*), inflammation (*Cd68*, *Lgals3*), fibrosis (*Lox*, *Timp-1, Nox4, Ctgf*) and heart function (*Serca2a*, *Nppa*) was determined by Sybr Green based Real Time qPCR (95°C 10 sec, 60°C 30 sec, 72°C 20 sec, 45 cycles followed by melting curve analysis) on the Roche Lightcycler 480 (Roche diagnostics Ltd., UK). *Gapdh* was used as a reference gene, since the expression of this gene did not differ between different muscles and mouse strains or over time. Primer efficiencies were determined and analysis was performed with LinREgPCR version 11.1 (Ramakers et al. 2003).

Statistics

Statistical analyses were performed with statistical software in R (package 2.11.1) and SPSS 17.0.2. (SPSS, Inc., Chicago, IL, USA). Cox regression analysis was used to test for differences in survival between groups (Fig. 1C and 2D). Figures 1, 3, 5 and 7 summarize the data, i.e. showing the mean and standard error of the mean per genotype and age. We applied an analysis of covariance (ANCOVA) to the temporal functional performance and CK level data, to overcome applying separate tests for each age between genotypes as this suffers from multiple testing and ignores the age trend. Age was used as a continuous variable and genotype as a categorical variable. Comparisons between *mdx/utrn*$^{-/-}$ mice with the other strains were performed on data obtained between the age of 4 and 11 weeks, while for comparisons between the other strains, data from all ages was taken into account. In choosing the appropriate model we applied the principle of parsimony. Given the application of tests for several different variables, we considered $P<0.01$ as significant. A one-way ANOVA was used to analyze the serum biomarkers, the percentage of fibrosis, central nucleation and the gene expression data, followed by the Bonferroni post-hoc test in case of significance. For the fiber size distributions, the one-way ANOVA test was applied on the median of all fibers of each mouse and in case of significance ($P<0.05$) followed by a Bonferroni post hoc test. Spearman correlation was used to test for correlations. The heart function data were analyzed with the one-way ANOVA in case of significance ($P<0.05$) a LSD post hoc test was applied. For all these tests a $P<0.05$ was considered significant.

Results

Low dystrophin levels improve muscle function

Mdx/utrn$^{-/-}$*/Xist*$^{\Delta hs}$ females were bred and used to study the potential of low dystrophin levels to improve motor function in the absence of utrophin (fig. 1A). *Mdx/utrn*$^{-/-}$*/Xist*$^{\Delta hs}$ (n = 20) and *mdx/utrn*$^{-/-}$ (n = 9) mice underwent a functional test regime consisting of four different tests per week for a maximum of 12 weeks (van Putten et al. 2010). Mice were sacrificed when the burden of the phenotype was moderate/severe, or at completion of the functional test regime (aged 16 weeks). Post mortem dystrophin levels of the quadriceps were determined by western blot. No dystrophin was observed for *mdx/utrn*$^{-/-}$ mice, while for *mdx/utrn*$^{-/-}$*/Xist*$^{\Delta hs}$ mice levels varied between 3-16.2% (fig. 1B). In cross-sections of *mdx/utrn*$^{-/-}$*/Xist*$^{\Delta hs}$ mice, dystrophin co-localized with β-dystroglycan, suggesting that the dystrophin-glycoprotein complex was restored (For a representative see picture fig. S1A).

Mdx/utrn$^{-/-}$*/Xist*$^{\Delta hs}$ mice were divided into two groups based on dystrophin levels either below or above the median dystrophin level observed (3.9%). Most strikingly, 14 out of 20 *mdx/utrn*$^{-/-}$*/Xist*$^{\Delta hs}$ mice survived the entire test period, while none of the *mdx/utrn*$^{-/-}$ mice did (P<0.0001, fig. 1C). Mice with >4% dystrophin outlived mice with <4% dystrophin (P<0.001).

Creatine kinase (CK) levels reduced in a dystrophin level dependent manner (fig. 1D). Mice with >4% dystrophin had lower CK levels than mice with <4% dystrophin (average 2604 U/L vs 3860 U/L, P<0.05), but levels did not completely normalize to wild type (<500 U/L, P<0.0001).

Maximum times obtained in the two limb hanging wire test for *mdx/utrn*$^{-/-}$*/Xist*$^{\Delta hs}$ mice were higher than those for *mdx/utrn*$^{-/-}$ mice (>4% 404 sec and <4% 298 sec, vs 71 sec for *mdx/utrn*$^{-/-}$, P<0.0001, fig. 1E). Mice with >4% dystrophin outperformed mice with <4% dystrophin (P<0.01). However, performance was not completely restored to wild type (594 sec, P<0.0001). A similar pattern was obtained for the four limb hanging wire test, in which all *mdx/utrn*$^{-/-}$*/Xist*$^{\Delta hs}$ mice outperformed *mdx/utrn*$^{-/-}$ mice (>4% 496 sec and <4% 407 sec, vs 163 sec for *mdx/utrn*$^{-/-}$, P<0.01, fig. 1F). Expression of >4% dystrophin improved outcome over <4% dystrophin (P<0.001), but did not completely restore it to wild type (586 sec, P<0.001). Normalized forelimb grip strength of *mdx/utrn*$^{-/-}$*/Xist*$^{\Delta hs}$ mice was greater than *mdx/utrn*$^{-/-}$ mice (>4% 59 grams and <4% 58 grams, vs 38 gram for *mdx/utrn*$^{-/-}$, P<0.0001), and lower than wild type mice (79 grams, P<0.0001, fig. 1G). *Mdx/utrn*$^{-/-}$*/Xist*$^{\Delta hs}$ mice outperformed *mdx/utrn*$^{-/-}$ mice on the rotarod (>4% 260 sec and <4% 222 sec, vs 51 sec for *mdx/utrn*$^{-/-}$, P<0.0001, fig. 1H), but performance did not differ between them. In our experience, wild type mice (*Xist*$^{\Delta hs}$ and C57BL/10ScSnJ) do not perform well on the rotarod (van Putten et al. 2012a;van Putten et al. 2012b). *Xist*$^{\Delta hs}$ mice ran longer than *mdx/utrn*$^{-/-}$ mice (183 sec vs 51 sec, P<0.0001), but shorter than *mdx/utrn*$^{-/-}$*/Xist*$^{\Delta hs}$ mice. In summary, for all functional tests, <4% dystrophin already substantially improves motor function compared to *mdx/utrn*$^{-/-}$ mice, while >4% dystrophin further improves hanging performance.

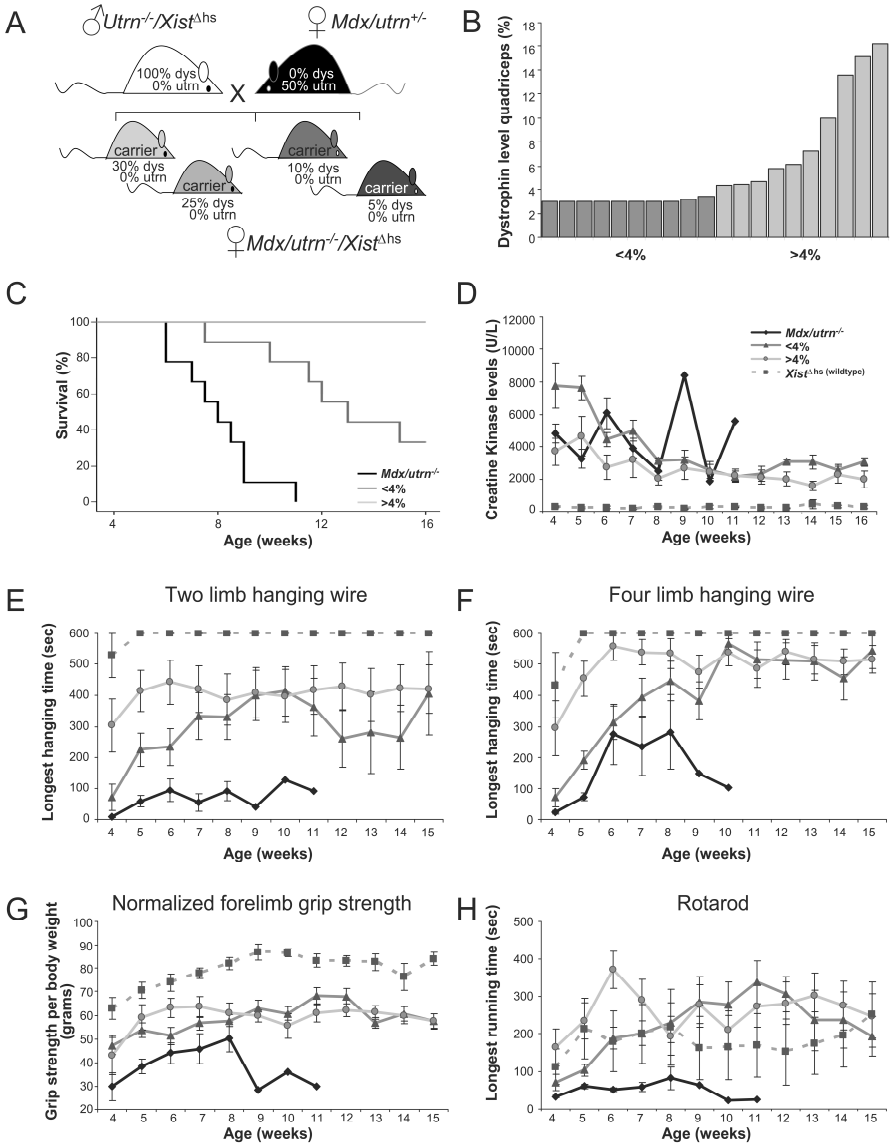

Fig. 1. Survival and functional performance of *mdx/utrn*$^{-/-}$/*Xist*$^{\Delta hs}$ mice. (**A**). *Mdx/utrn*$^{-/-}$ females expressing low dystrophin levels due to skewed X-inactivation were bred by crossing *utrn*$^{-/-}$/*Xist*$^{\Delta hs}$ males with *mdx/utrn*$^{+/-}$ females. (**B**). *Mdx/utrn*$^{-/-}$/*Xist*$^{\Delta hs}$ mice were grouped based on dystrophin levels of the quadriceps, which varied between 3 and 16.2%. (**C**). Levels <4% dystrophin increased life span in *mdx/utrn*$^{-/-}$/*Xist*$^{\Delta hs}$ mice (P<0.0001), while all *mdx/utrn*$^{-/-}$ mice died prematurely. Expression of >4% dystrophin prevented premature death. (**D**). CK levels decreased in a dystrophin level dependent manner in *mdx/utrn*$^{-/-}$/*Xist*$^{\Delta hs}$ mice, but did not completely normalize to wild type levels. (**E**). *Mdx/utrn*$^{-/-}$/*Xist*$^{\Delta hs}$ mice outperformed *mdx/utrn*$^{-/-}$ mice in the two limb hanging wire test, but performed worse compared to wild type mice (P<0.0001). >4% dystrophin resulted in better hanging times than <4% dystrophin (P<0.01). (**F**). *Mdx/utrn*$^{-/-}$/*Xist*$^{\Delta hs}$ mice hang longer compared to *mdx/utrn*$^{-/-}$ mice in the four limb hanging wire test. Expression of >4% dystrophin further increased performance (P<0.001), although it was worse than wild type mice (P<0.001). (**G**). *Mdx/utrn*$^{-/-}$/*Xist*$^{\Delta hs}$ mice had a greater forelimb grip strength than *mdx/utrn*$^{-/-}$ mice (P<0.0001). (**H**). Rotarod running times of *mdx/utrn*$^{-/-}$/*Xist*$^{\Delta hs}$ mice exceeded those of *mdx/utrn*$^{-/-}$ and wild type mice (P<0.0001). Data are represented as mean±SEM.

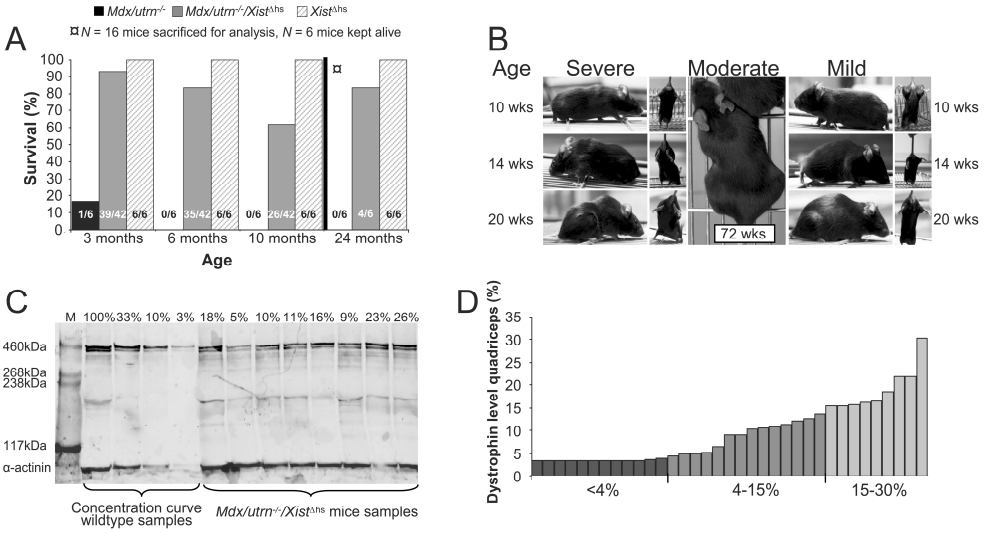

E

	Phenotype			
Dys level		Severe	Moderate	Mild
	<4%	46%	23%	23%
	4-15%	7%	28%	64%
	15-30%	0%	0%	100%

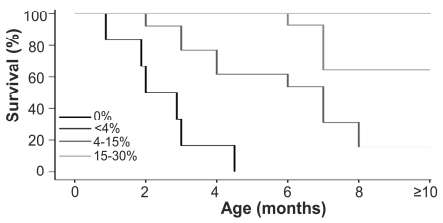

G

Mouse	Dys level	Phenotype	Life span (months)	Cause of death
1	3%	Severe	17	Muscular dystrophy
2	27%	Moderate	24.5	Muscular dystrophy
3	35%	Mild	17.5	Black gall bladder, pale liver
4	55%	Mild	25.7	Agressive tumor
5	N.D.	Mild	25	Natural cause; ageing
6	N.D.	Mild	26	Alive at time of submission

Fig. 2. Long term survival of *mdx/utrn*$^{-/-}$*/Xist*$^{\Delta hs}$ mice. (**A**). *Mdx/utrn*$^{-/-}$*/Xist*$^{\Delta hs}$ mice significantly outlived *mdx/utrn*$^{-/-}$ mice, which all died prematurely, as at the age of 10 months, 26 out of 42 mice were still alive. Sixteen mice were sacrificed for analysis before the age of one year and six mice were allowed to life, of which four were still alive at the age of two years. (**B**). *Mdx/utrn*$^{-/-}$*/Xist*$^{\Delta hs}$ mice could be discriminated into three phenotypically distinct groups based on disease severity. Severely affected mice developed similar symptoms as *mdx/utrn*$^{-/-}$ mice although at a much older age. Moderately affected mice developed malformations of the hips possibly combined with kyphosis, while mildly affected mice were similar to wild type mice. (**C**). Representative western blot of the quadriceps. The percentage of individual mice was assessed using a concentration curve made from wild type samples. (**D**). Dystrophin levels of the quadriceps ranged from 3-30.4%, which was used to divide mice into three groups. (**E**). Dystrophin expression correlated to the phenotype of the mice. (**F**). Dystrophin expression correlated to phenotypic appearance and life span (R=0.718 $P<0.0001$). Levels of <4% dystrophin improved life span, with 63% of these mice still alive at the age of 6 months ($P<0.01$). Expression of higher dystrophin levels further improved life span. (**G**) Overview of the dystrophin levels of the quadriceps, clinical features, life span and cause of death of six *mdx/utrn*$^{-/-}$*/Xist*$^{\Delta hs}$ mice that were kept alive. Data are represented as mean.

Dystrophin levels of <4% improve long term survival

To more thoroughly investigate life span of *mdx/utrn*$^{-/-}$*/Xist*$^{\Delta hs}$ mice, a longer survival study was performed in 42 *mdx/utrn*$^{-/-}$*/Xist*$^{\Delta hs}$ and 6 *mdx/utrn*$^{-/-}$ mice. Several other aspects of skeletal muscle and heart function were assessed along with histopathology. *Mdx/utrn*$^{-/-}$ mice again became severely affected as they developed kyphosis, could not spread their hindlimbs and had difficulties moving and breathing, leading to death generally before the age of 12 weeks (fig. 2A). Disease severity of *mdx/utrn*$^{-/-}$*/Xist*$^{\Delta hs}$ mice could be divided into three phenotypically distinct subgroups (fig. 2B). The first subgroup developed similar symptoms as *mdx/utrn*$^{-/-}$ mice, including severe muscle weakness, kyphosis and inability to spread their hindlimbs. Notably, these mice exhibited these pathological features at an older age than *mdx/utrn*$^{-/-}$ mice and had a similar appearance to wild type mice before onset. Mice of the second subgroup had a moderate phenotype; they developed malformations of the hips, leading to an unnatural way of walking (video available on request). This was observed either in presence or absence of kyphosis. The last subgroup exhibited a mild phenotype and appeared comparable to wild type mice. The age of death depended on the age at onset of pathology and the degree of severity. Generally, mice with a moderate or mild phenotype outlived those with a severe phenotype.

For each mouse studied, post mortem dystrophin levels of the quadriceps were determined by western blot (fig. 2C). Levels varied between 3-30.4% and were higher than those observed for animals sacrificed after 16 weeks. We attribute this to selection of dystrophin positive fibers over time (Danko et al. 1992;Karpati et al. 1990), or transcriptional rate exceeding protein turnover rate, causing accumulation of protein over time. Based on the dystrophin level, mice were divided into three groups (fig 2D). *Mdx/utrn*$^{-/-}$*/Xist*$^{\Delta hs}$ mice belonging to the severe phenotype mostly had <4% dystrophin (fig 2E). Of these, 62% were still alive at the age of 6 months, reflecting an improved life span compared to *mdx/utrn*$^{-/-}$ mice (P<0.01). Dystrophin levels between 4-15% generally resulted in a moderate or mild phenotype and increased survival compared to *mdx/utrn*$^{-/-}$ mice (P<0.0001). Of these mice 100% were still alive after 6 months and 64% after 10 months (fig 2F). Notably, their life span was further improved over the mice with <4% dystrophin (P<0.01). All mice with 15-30% dystrophin survived until the age of 10 months after which they were sacrificed for analysis, extending their life span yet further than all other mice (P<0.05). The Spearman correlation test confirmed a very strong positive correlation between dystrophin expression and life span (R=0.718 P<0.0001).

Six *mdx/utrn*$^{-/-}$*/Xist*$^{\Delta hs}$ mice were kept alive (fig 2G). At the time of submission, one mouse aged 26 months, is still alive, looking similar to age-matched wild type mice. Three out of the five remaining mice died of non-muscle related causes, aged 17.5, 25 and 25.7 months and expressing >35% dystrophin. The other two mice died as a consequence of their muscular dystrophy aged 17 (fig. S1B) and 24.5 months (fig. S1C). These mice had a severe and moderate phenotype and expressed 3% and 27% dystrophin respectively.

Low dystrophin levels improve muscle function and normalize serum biomarker levels

During the survival study, all mice were subjected to two limb hanging wire and forelimb grip strength tests once every 6 weeks (van Putten et al. 2010). Hanging performance clearly depended on dystrophin expression. Mice with <4% dystrophin hung shorter than mice with 4-15% dystrophin (135 vs 369 sec, P<0.0001, fig 3A), while mice with 15-30% dystrophin hung even longer (499 sec, P<0.01). Forelimb grip strength of mice with <4% dystrophin was lower than that of mice with 4-15% dystrophin (55 grams vs 60 grams, P<0.05, fig. 3B), which were as strong as mice with 15-30% dystrophin (63 grams, P=0.16).

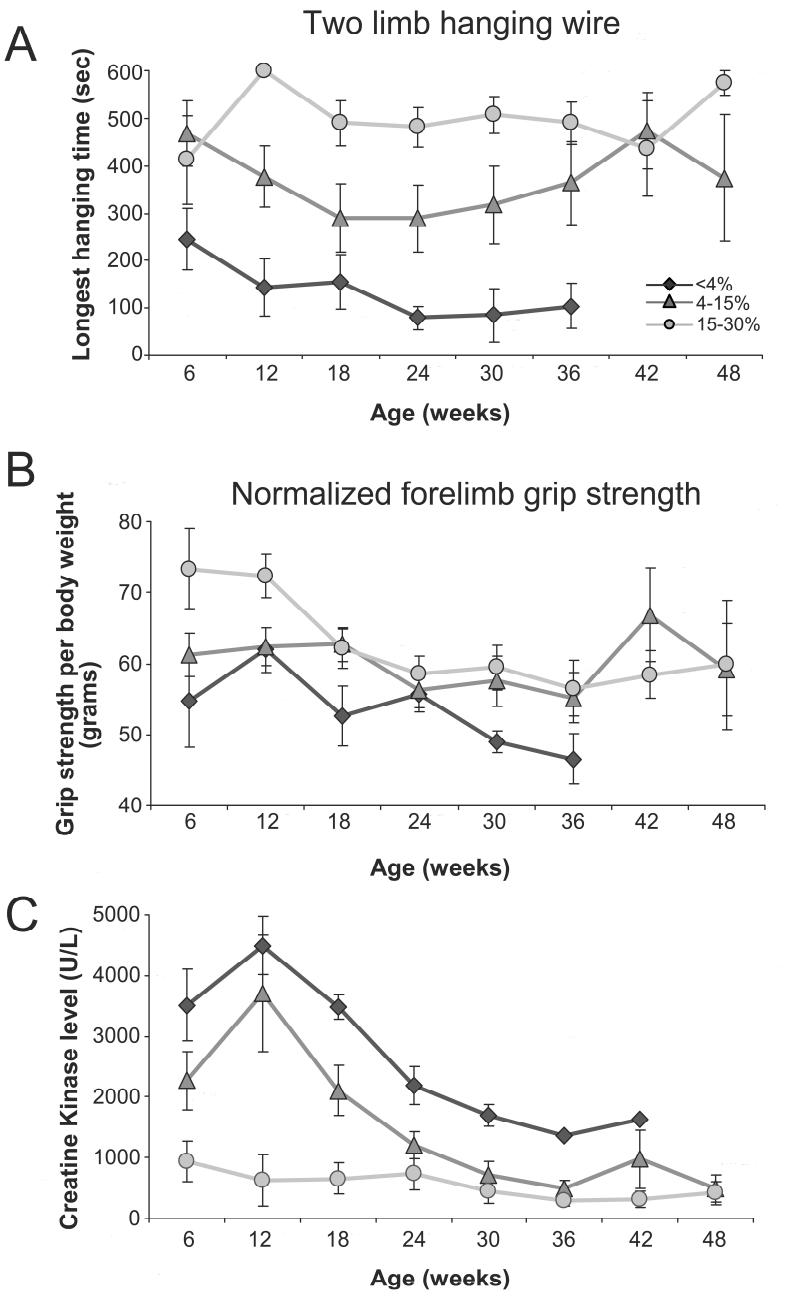

Fig. 3. Functional performance and plasma CK levels. (**A**). Two limb hanging wire performance was impaired in mice with <4% dystrophin compared to mice with 4-15% dystrophin (P<0.001), and mice expressing 15-30% dystrophin (P<0.001). (**B**). Mice with 4-15% dystrophin had a larger normalized forelimb grip strength than mice with <4% dystrophin (P<0.05). Strength did not further improve in mice with 15-30% dystrophin. (**C**). CK levels were elevated in mice with <4% dystrophin compared to mice with >4% dystrophin. For all mice, levels dropped over time and reached wild type levels from 30 weeks of age onwards. Data are represented as mean±SEM.

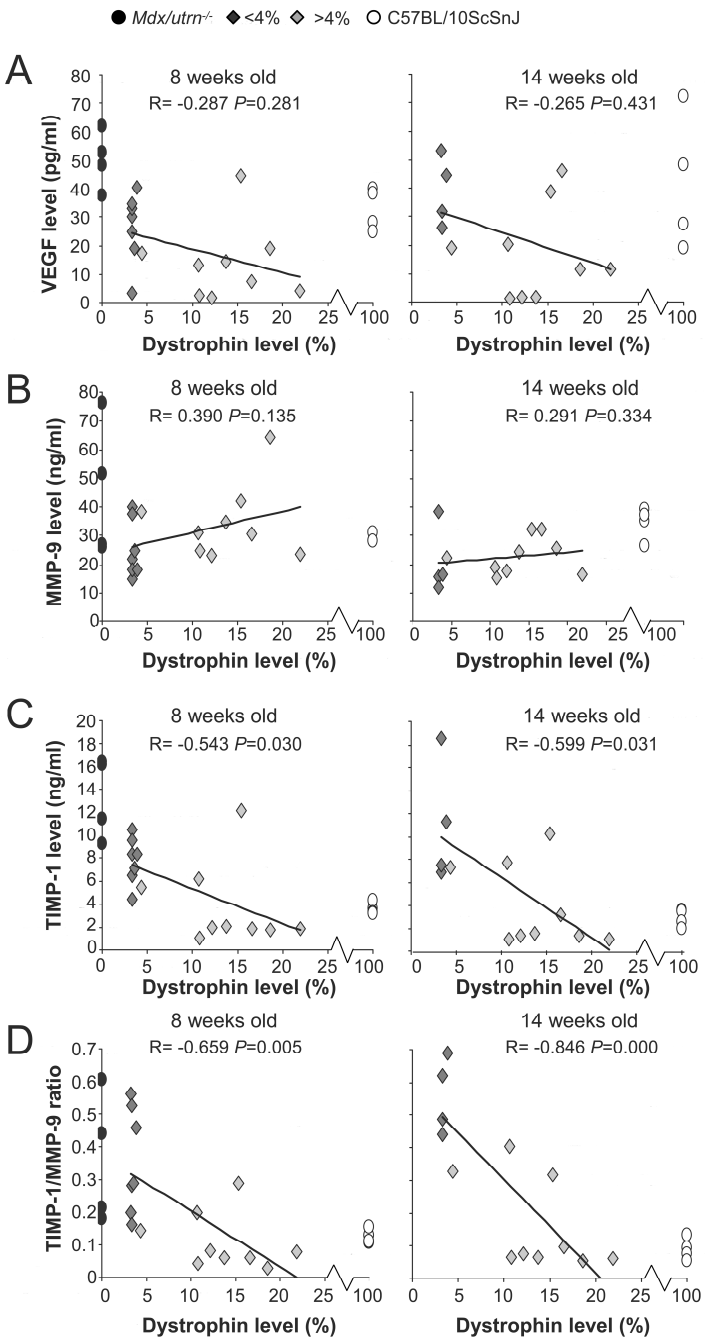

Fig. 4. Serum levels of VEGF, MMP-9 and TIMP-1 at 8 and 14 weeks of age. (**A**). VEGF levels already decreased in mice with <4% dystrophin. (**B**). MMP-9 levels normalized in mice with <4% dystrophin. (**C**). TIMP-1 levels showed a clear dystrophin level dependent normalization. Already <4% dystrophin decreased levels compared to *mdx/utrn*$^{-/-}$ mice while >4% dystrophin resulted in further decrement. (**D**). The TIMP-1/MMP-9 ratio normalized to wild type levels in mice with >4% dystrophin.

Plasma CK levels, assessed every 6 weeks throughout the study, clearly fell in all mice over time. Mice with <4% dystrophin had higher CK levels than mice with 4-15% dystrophin (3251 vs 1785 U/L, $P<0.0001$, fig. 3C). CK levels fell further in mice with 15-30% dystrophin, reaching wild type levels from 30 weeks onwards (554 U/L, $P<0.0001$).

Serum levels of VEGF (angiogenesis (Saito et al. 2009)), MMP-9 and TIMP-1 (tissue integrity (Nadarajah et al. 2011;van Putten et al. 2012a)) were analyzed on a group of 20 *mdx/utrn*$^{-/-}$/*Xist*$^{\Delta hs}$, 4 *mdx/utrn*$^{-/-}$ and 4 C57BL/10ScSnJ mice at the age of 8 and 14 weeks (fig. 4). Levels of all biomarkers were elevated in *mdx/utrn*$^{-/-}$ compared to wild type mice. At 8 weeks, VEGF levels were already decreased with < 4% dystrophin ($P<0.05$), whereas >4% dystrophin also normalized TIMP-1 and the TIMP-1/MMP-9 ratio to wild type levels. At 14 weeks, <4% dystrophin decreased VEGF and MMP-9 levels, whereas >4% dystrophin also normalized TIMP-1 levels and the TIMP-1/MMP-9 ratio. At both ages, dystrophin expression significantly correlated to TIMP-1 levels (8 weeks R= -0.543 $P=0.03$, 14 weeks R= -0.599 $P=0.03$) and the TIMP-1/MMP-9 ratio (8 weeks R= -0.659 $P=0.005$, 14 weeks R= -0.846 $P<0.001$).

Low dystrophin levels improve muscle pathology

A strong negative correlation was observed between dystrophin expression and the percentage of fibrosis and necrosis (R= -0.616 $P<0.0001$, fig. 5A). *Mdx/utrn*$^{-/-}$/*Xist*$^{\Delta hs}$ mice with <4% dystrophin had more fibrosis and necrosis than *mdx/utrn*$^{-/-}$ mice ($P<0.05$). This is possibly due to the age difference of the two groups (6-9 weeks and 7-40 weeks). Levels of fibrosis and necrosis dropped in mice expressing >4% dystrophin ($P<0.01$) and did not differ from wild type levels.

Fiber size distribution and the percentage of centrally nucleated fibers also normalized towards wild type levels in a dystrophin level dependent manner in mice expressing >4% dystrophin (fig. 5B-C). Dystrophin expression also correlated to the median of fiber surface area (R=0.779 $P<0.0001$) and central nucleation (R= -0.675, $P<0.0001$).

Finally, we quantified the expression of some biomarker genes involved in inflammation (*Cd68*, *Lgals3*), fibrosis (*Lox*, *Timp-1*) and regeneration (*eMHC3*, *Myog*) for the quadriceps (fig. 5D-F). Although the high inter group variation only occasionally resulted in significant differences, there is a clear pattern, in line with the histological data, that gene expression of *mdx/utrn*$^{-/-}$/*Xist*$^{\Delta hs}$ mice with <4% dystrophin is higher than *mdx/utrn*$^{-/-}$ mice, while >4% dystrophin results in a clear dystrophin level dependent normalization towards wild type levels.

Dystrophin level dependent improvement of heart pathology

At the age of 10 months, heart function of *mdx/utrn*$^{-/-}$/*Xist*$^{\Delta hs}$ mice ($n = 10$) was analyzed with Magnetic Resonance Imaging and compared with age and gender-matched *mdx*, *Xist*$^{\Delta hs}$ and C57BL/10ScSnJ mice ($n = 5$). Dystrophin levels of the heart ranged from 2.5-49.2% (median = 13.7, *stdev* = 17.3) and mice were divided into a low (2.5-10.9%, median = 4.3, *stdev* = 3.3), and high dystrophin level group (16.4-49.2%, median = 29.7, *stdev* = 14.3). Left ventricular ejection fraction of mice with low dystrophin levels was severely hampered, but improved in mice expressing higher dystrophin levels ($P<0.05$), although not to wild type levels ($P<0.01$, fig. 6).
Also stroke volume was significantly decreased ($P<0.05$) in all *mdx/utrn*$^{-/-}$/*Xist*$^{\Delta hs}$ mice. Right ventricular function was not affected in *mdx/utrn*$^{-/-}$/*Xist*$^{\Delta hs}$ mice. Dystrophin expression correlated to the ejection fraction of both ventricles (left R=0.817 $P=0.007$, right R=0.717 $P=0.03$).

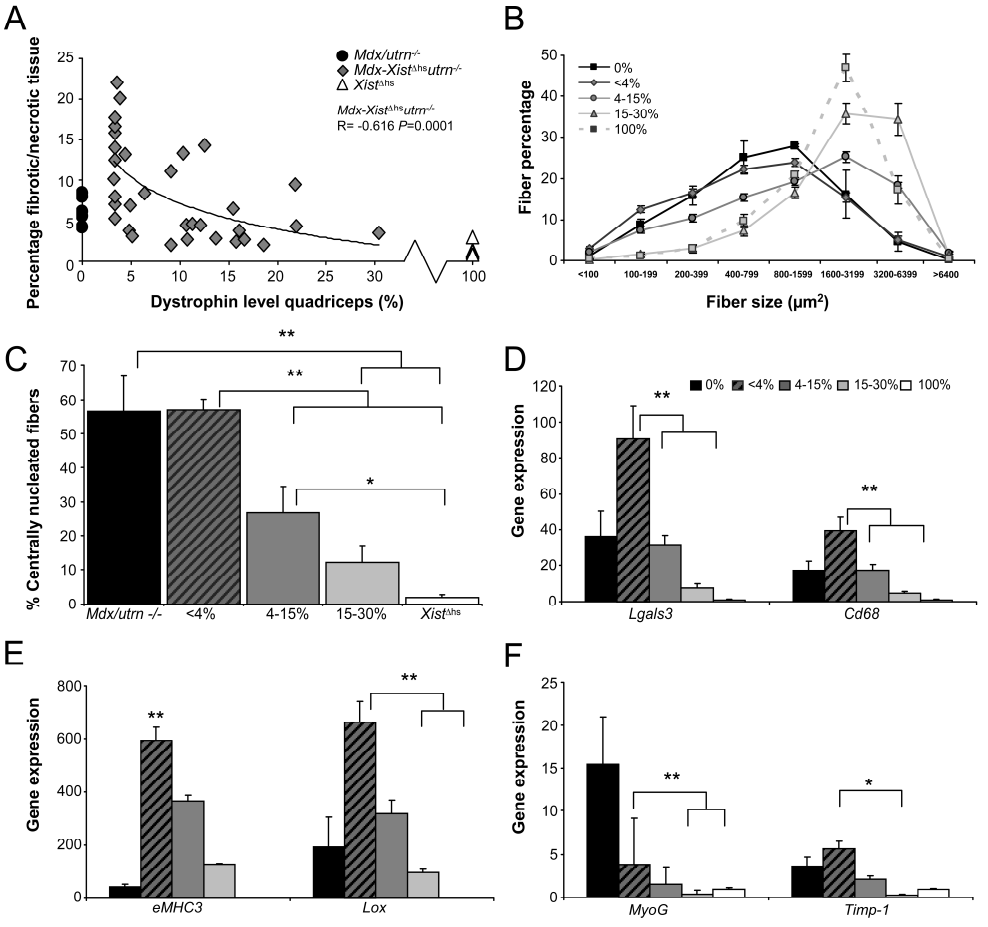

Fig. 5. Dystrophin levels and histopathology. Note that not all mice are of similar age; *mdx/utrn*$^{-/-}$ mice did not live beyond 12 weeks, while the age of *mdx/utrn*$^{-/-}$*/Xist*$^{\Delta hs}$ mice ranges from 7 weeks to 1 year. Data of *Xist*$^{\Delta hs}$ mice are from 16 week old animals. (**A**). Dystrophin expression negatively correlated to the percentage of fibrotic/necrotic tissue (R= -0.518 *P*<0.002). Mice with <4% dystrophin had more fibrotic/necrotic tissue compared to *mdx/utrn*$^{-/-}$ mice (*P*<0.05). (**B**). Fiber size distribution of mice with <4% dystrophin was comparable to that of *mdx/utrn*$^{-/-}$ mice, whereas 4-15% dystrophin reduced the number of small recently regenerated fibers. Distribution pattern of mice with 15-30% dystrophin closely resembled that of wild type mice. (**C**). Central nucleation was comparable for *mdx/utrn*$^{-/-}$ mice and mice with <4% dystrophin. Higher dystrophin levels resulted in a drop (*P*<0.01) although levels were still considerably higher than wild type. (**D-F**). Expression levels of genes involved in inflammation (*Lgals3, Cd68*), regeneration (*eMHC3, Myog*) and fibrosis (*Lox, Timp-1*) were upregulated in mice with <4% dystrophin compared to *mdx/utrn*$^{-/-}$ mice, whereas a dystrophin level dependent normalization was observed for the other groups. Single and double asterisks represent a *P*-value of <0.05 and <0.01 respectively. Data are represented as mean±SEM.

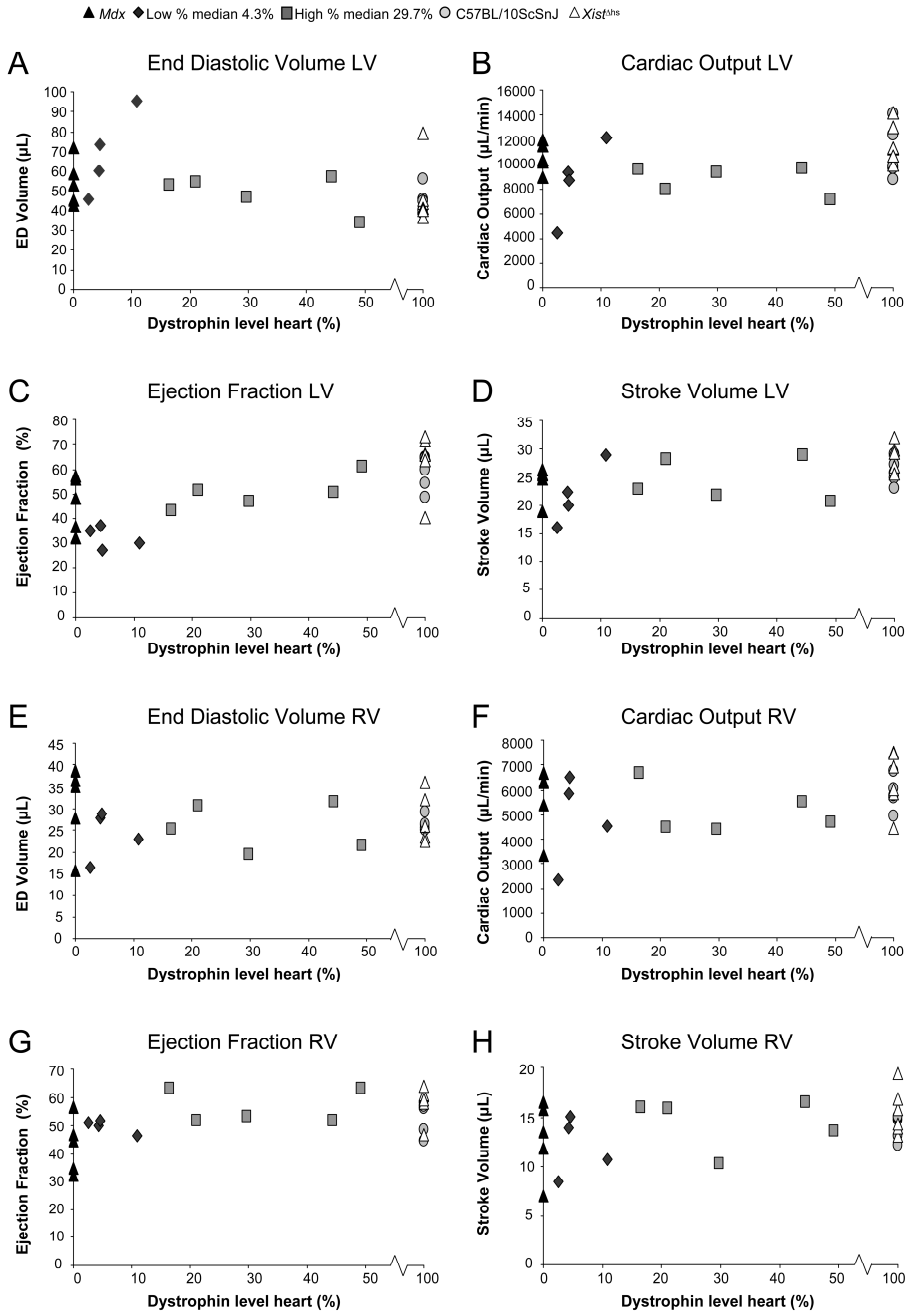

Fig. 6. Heart function. (**A-D**). Heart function of the left ventricle (LV). Ejection fraction and stroke volume of *mdx/utrn*$^{-/-}$*/Xist*$^{\Delta hs}$ mice with low dystrophin levels were severely hampered. This was restored by expression of high dystrophin levels, although not completely to wild type levels. (**E-H**). Heart function of the right ventricle (RV) was not affected in any of the *mdx/utrn*$^{-/-}$*/Xist*$^{\Delta hs}$ mice. Ejection fraction of *mdx* mice was significantly (P<0.05) smaller than that of wild type strains and mice with high dystrophin levels.

Dystrophin expression also negatively correlated to the extent of fibrosis (R= -0.733 $P<0.05$). The extensive fibrosis in mice with low dystrophin levels was markedly reduced in mice with higher levels of dystrophin ($P<0.05$, fig. 7A and S1D) although still exceeding wild type ($P<0.01$).

Expression of genes involved in inflammation, fibrosis and heart function was elevated in hearts of all dystrophic mice compared to wild type, except for *Serca2a*, of which levels are known to be down regulated in dystrophic mice (fig. 7B). In line with the histological data, gene expression levels of mice high dystrophin levels was normalized, although still exceeded wild type levels.

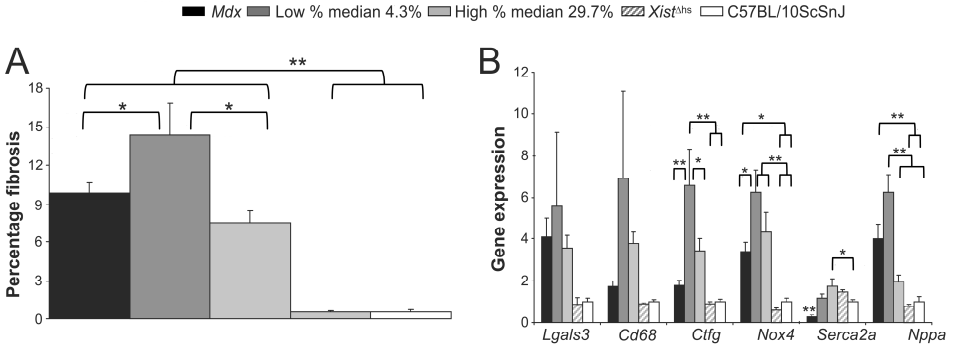

Fig. 7. Heart pathology. (**A**). The percentage of fibrotic tissue in mice with low dystrophin levels was higher than mice with higher dystrophin levels and *mdx* mice ($P<0.05$). Wild type mice had lower levels compared to dystrophic mice ($P<0.01$). (**B**). Expression of genes involved in heart pathology and function matched that found for histopathology. Gene expression of *mdx/utrn*$^{-/-}$*/Xist*$^{\Delta hs}$ mice with low dystrophin levels was higher compared to those of mice with higher dystrophin levels, *mdx* and wild type mice. Single and double asterisks represent a *P*-value of <0.05 and <0.01 respectively. Data are represented as mean±SEM.

Discussion

Over the last couple of years, several therapeutic strategies for DMD have progressed into clinical trials, aiming to restore functional dystrophin (Cirak et al. 2011;Goemans et al. 2011;Malik et al. 2010;Bowles et al. 2011;Skuk et al. 2006). Most likely, these strategies will not result in full restoration of dystrophin to healthy control levels. However, based on the mild disease of BMD patients and DMD/BMD carriers expressing low dystrophin levels, this is probably not necessary to provide benefit,

Our study describes the *mdx/utrn*$^{-/-}$*/Xist*$^{\Delta hs}$ mouse, which expresses a variety of low dystrophin levels in a utrophin negative background based on skewed X-inactivation. In these mice, <4% of the wild type dystrophin level already greatly improved life span and performance in functional tests. Higher dystrophin levels (4-15%) yet further increased survival and functional performance in hanging wire tests, but not in grip strength and rotarod running. This suggests that maintenance of vitality and functionality of the front and hind paw musculature requires less dystrophin than the larger limb and trunk muscles do.

Over time, *mdx/utrn*$^{-/-}$*/Xist*$^{\Delta hs}$ mice expressing <4% dystrophin develop severe pathology, with high levels of fibrosis, central nucleation and upregulation of genes involved in pathology . We attribute the fact that the pathology of *mdx/utrn*$^{-/-}$ mice was in fact less severe, to the lack of time to develop more severe muscle damage prior to their early death (van Putten et al. 2012b). Thus, while expression of <4% dystrophin allowed for a longer life span and improved muscle function, it could not yet prevent severe muscle damage. In contrast, expression of >4% dystrophin, besides further improving life span and muscle function, also protected muscles against damage.

We also assessed the potential of several biomarkers to monitor disease progression over time. Although plasma CK levels decreased in a dystrophin dependent manner in *mdx/utrn*$^{-/-}$*/Xist*$^{\Delta hs}$ mice, they reached wild type levels after 30 weeks, hampering the usefulness of this biomarker. Both serum TIMP-1 levels and the TIMP-1/MMP-9 ratio correlated to dystrophin expression and showed a clear dystrophin level dependent normalization towards wild type levels. We therefore propose these as useful biomarkers to monitor therapeutic effects for dystrophin-restoring approaches in mice and possibly humans (Nadarajah et al. 2011). Although levels of MMP-9 and VEGF were elevated in *mdx/utrn*$^{-/-}$ compared to wild type mice, levels in *mdx/utrn*$^{-/-}$*/Xist*$^{\Delta hs}$ mice were similar to, or lower than wild type mice. This implies that, at least in mice, MMP-9 and VEGF are less suitable serum biomarkers.

Ten-month-old *mdx/utrn*$^{-/-}$*/Xist*$^{\Delta hs}$ mice expressing low dystrophin levels (median 4.3%) suffered from a more severe cardiomyopathy than mice expressing higher dystrophin levels (median 29.7%). This suggests that prolonged life span and functionality in these mice leads to a high workload for which the lower dystrophin levels in the heart can not entirely compensate. A small limitation of this experiment is that the scans only entirely covered the left ventricle, which was our main focus at initiation of the study. Interesting findings published on the right ventricle meanwhile encouraged us to also analyze this ventricle. Comparability was ensured by analyzing all scans in the same manner and exactly to the same height. However, as the top part of the right ventricle was not scanned and measured, this resulted in a lower cardiac output, and underestimation of end diastolic volume. This may also explain that in this study the left ventricle was more severely affected, while others have reported the opposite (Crisp et al. 2011;Verhaart et al. 2011).

It should be noted that *mdx/utrn*$^{-/-}$*/Xist*$^{\Delta hs}$ mice have low dystrophin levels in a mosaic manner from birth onwards, protecting them during extensive cycles of regeneration and degeneration occurring early in life. Studies treating *mdx/utrn*$^{-/-}$ mice postnatally are limited to a starting age of at least 10 days (Goyenvalle et al. 2010;Goyenvalle et al. 2012;Kawano et al. 2008). Generally, dystrophin levels needed to improve life span exceeded 25% in these studies. We observe that 4-15% dystrophin not only greatly improves life span and muscle function, but also prevents histopathological damage. This indicates that, at least in mice, dystrophin restoration has larger protective effects when initialized very early after birth, or even before. Whether similar effects on disease pathology can also be expected for DMD patients is unknown.

To summarize, the *mdx/utrn*$^{-/-}$*/Xist*$^{\Delta hs}$ mouse model described here expresses a range of low dystrophin levels in a utrophin negative background. Major improvement in life span and functional performance is obtained even with expression of <4% dystrophin, while further improvement in life span and performance as well as protection against muscle damage is achieved when >4% dystrophin is expressed. These data indicate that very low dystrophin levels, like they are currently generated in several therapeutic trials, may already have substantial beneficial effects in DMD patients, which is encouraging for therapies aiming at dystrophin restoration. Especially worth noting is the striking effect on survival. This is probably due to general effects on condition and resilience, which are not otherwise measurable so far. If this pertains to DMD in humans as well, extension of the life span may be amongst the main benefits of therapies currently in development. This puts special emphasis of the urgent need to develop additional, and more refined therapeutic readouts than those based on ambulation.

Acknowledgements

We thank prof. Neil Brockdorff and dr. Tatyana Nesterova (MRC Clinical Sciences Center, London, UK, current affiliation Department of Biochemistry, University of Oxford, UK) for the *Xist*$^{\Delta hs}$ embryos and help with genotyping the mice, and prof. Kay Davies (Department of Physiology, Anatomy and Genetics, University of Oxford) for providing us with the *mdx/utrn*$^{-/-}$ mouse. We are grateful to Maarten van Iterson and Jelle Goeman for their help with statistical analyses. **Funding:** This work is supported by the FP6 funded TREAT-NMD network of excellence (LSHM-CT-2006-036825), the Dutch organization for scientific research (NWO/ZonMW, grant number 43200002), and the Dutch Duchenne Parent Project and utilizes the infrastructure of the Center for Biomedical Genetics (the Netherlands) and the Center for Medical Systems Biology (the Netherlands). **Author contributions:** Conceived and designed the experiments: LVDW, PACH, GJBVO, AAR. Performed the experiments: MVP, MH, CY, VDN, HH. Analyzed the data: MVP, MH, VDN, AAR. Wrote the paper: MVP, AAR. **Competing interests:** The authors declare no conflict of interest. **Data and materials availability:** The data are archived in an approved database and will be available for every reader. The *Xist*$^{\Delta hs}$ model was shared by Neil Brockdorff; requests for sharing (MTA) should be addressed to him.

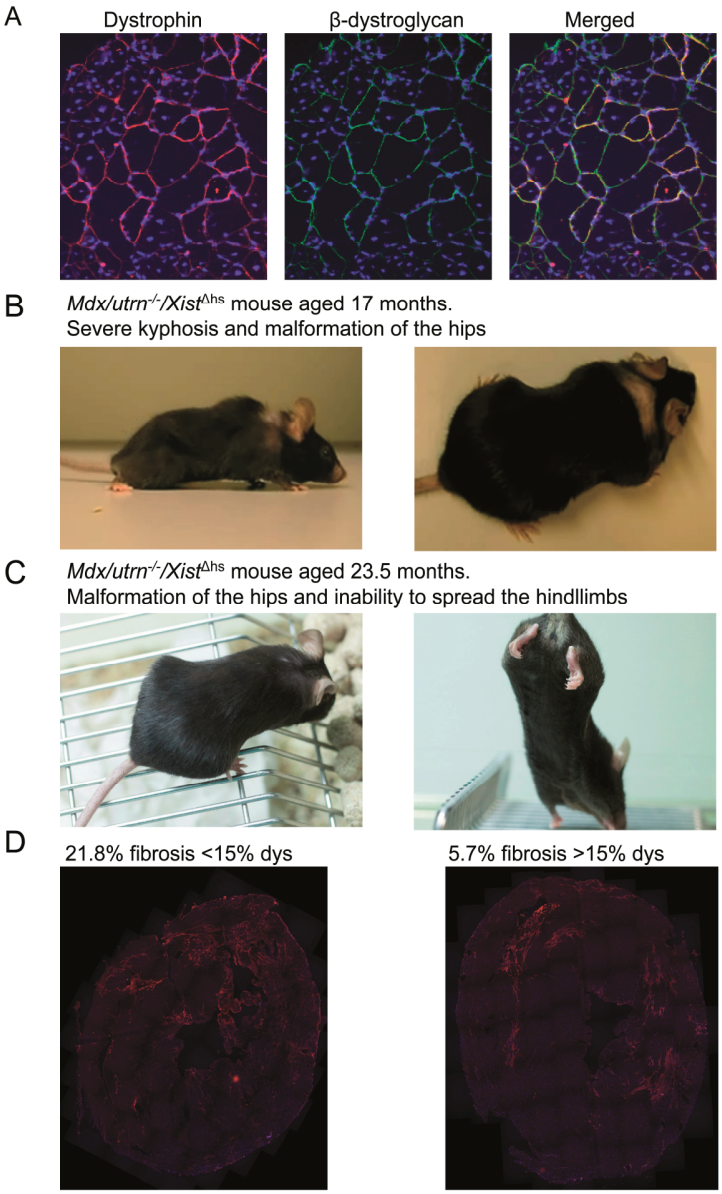

Fig. S1. Characterization of the *mdx/utrn*$^{-/-}$*/Xist*$^{\Delta hs}$ mouse. (**A**). Transverse cross-section of the quadriceps stained with dystrophin that nicely co-localizes with β-dystroglycan, a member of the dystrophin-associated protein complex. (**B**). *Mdx/utrn*$^{-/-}$*/Xist*$^{\Delta hs}$ mouse exhibiting severe kyphosis and malformations of the hips at the age of 17 months. Both phenotypical characteristics were developed later in life. This mouse was found dead at the age of 17 months, probably caused by respiratory or heart failure as body weight only slightly dropped in the week prior to death. This mouse expressed 3% dystrophin in the quadriceps. (**C**). *Mdx/utrn*$^{-/-}$*/Xist*$^{\Delta hs}$ mouse exhibiting a minor degree of kyphosis and severe malformations of the hips at the age of 23.5 months, which was developed later in life. This mouse was sacrificed at the age of 24.5 months, after it slowly but progressively lost weight. The mouse expressed 27% dystrophin in the quadriceps. (**D**). Representative pictures of a transverse cross-section of the heart stained with Collagen Type I from 10 months old *mdx/utrn*$^{-/-}$*/Xist*$^{\Delta hs}$ mice with either <15% or >15% dystrophin, which resulted in 21.8 and 5.7% fibrosis respectively.